COMPRESSIBILITY IMPACT ON THE AERODYNAMIC SURFACE QUANTITIES OF RAREFIED HYPERSONIC FLOW OVER FORWARD-FACING STEPS

Paulo H. M. Leite, phmineiro@lcp.inpe.br
Wilson F. N. Santos, wilson@lcp.inpe.br
Combustion and Propulsion Laboratory (LCP), Nacional Institute for Space Research (INPE), Cachoeira Paulista, SP 12630-000

Abstract. *Compressibility effects on hypersonic flow over forward-facing steps have been numerically investigated by using the Direct Simulation Monte Carlo (DSMC) method. The work is motivated by interest in assessing the impact of surface discontinuities on hypersonic configurations in the transition flow regime. The computations were carried out by assuming step frontal-face height from 3 to 5 millimeters and freestream Mach number from 5 to 25 at zero-degree angle of incidence. The results highlight some significant differences on the aerodynamic surface quantities due to variations on the step frontal-face height and on the freestream Mach number. Interesting features observed on pressure, skin friction, and heat transfer coefficients showed that small frontal-face thickness, compared to the freestream mean free path, still has important effects on these properties for the freestream Mach number range investigated.*

Keywords: *DSMC, Hypersonic Flow, Rarefied Flow, Forward-Facing Step.*

1. INTRODUCTION

It is generally recognized that the physical phenomena related to the problem of separation are very important in the design of hypersonic configurations. When separation occurs in high Mach number flows, the changes in pressure distribution and heat transfer rate can have catastrophic effects in the vehicle. The presence of hot spots at separation and reattachment points changes the characteristics of the flow over the vehicle and can cause failure in the thermal protection system, as was evidenced by the tragic loss of Space Shuttle Columbia in 2003. In general, separation occurs due to the interaction of external flows with various desired or undesired design features present on the vehicle surface, such as protuberances, notches, cavities, gaps, or steps.

For the particular case of steps, there is a rather extensive studies dealing with forward-facing step flows in the current literature. In general, these research studies have been conducted in order to understand, among others, the physical aspects of a laminar or turbulent boundary layer in a subsonic (Camussi *et al.*, 2008; Chapman *et al.*, 1958; Stüer et al., 1999), supersonic (Bogdonoff and Kepler, 1955; Chapman *et al.*, 1958; Driftmyer, 1973) or hypersonic (Grotowsky and Ballmann, 2000; Nestler *et al.*, 1969; Wilkinson and East, 1968) flow past to this type of discontinuity, characterized by a sudden change on the surface slope.

The major interest in these research studies on forward-facing step has gone into considering laminar or turbulent flow in the continuum flow regime. However, there is little understanding of the physical aspects of rarefied hypersonic flows past to steps related to the severe aerothermodynamic environment associated with a reentry vehicle. In this scenario, Leite and Santos (Leite and Santos, 2009a,b) have investigated forward-facing steps situated in a rarefied hypersonic flow by employing the Direct Simulation Monte Carlo (DSMC) method. The studies were motivated by the interest in investigating the frontal-face height effect on the flowfield structure and on the aerodynamic surface properties in the transition flow regime, i.e., between the continuum flow and the free collision flow regime. The analysis showed that the hypersonic flow past a forward-facing step was characterized by a strong compression ahead of the frontal face. The analysis also showed that disturbances upstream the step depended on changes in the frontal-face height of the steps. In addition, results showed that the separation point and the pre-separation region relied on the frontal-face height.

The present investigation was undertaken in an attempt to extend further the previous analysis (Leite and Santos,

2009a,b) by investigating the impact of the freestream Mach number on the aerodynamic surface quantities for a family of forward-facing step. In this scenario, the primary goal of this paper is to assess the sensitivity of the surface quantities, such as pressure, skin friction, and heat transfer coefficients, due to changes on the freestream Mach number and on the frontal-face height. A detailed and careful effort is made to provide a comprehensive description of the flow with special relevance to the particular case where the step height is less than the boundary-layer thickness. In addition, the focus of the present study is the low-density region in the upper atmosphere, where numerical gaskinetic procedures are available to simulate hypersonic flows. Therefore, the DSMC method will be employed to calculate the hypersonic two-dimensional flow on the steps.

2. GEOMETRY DEFINITION

Surface discontinuities present on reentry hypersonic configurations are modeled in this investigation by forward-facing steps as defined in the previous studies (Leite and Santos, 2009a,b). By considering the step frontal-face h is much smaller than the nose radius R of a reentry vehicle, i.e., $h/R \ll 1$, then the hypersonic flow over the step may be considered as a hypersonic flow over a flat plate with a forward-facing step. Figure 1(a) displays a schematic view of the model employed and presents the important geometric parameters.

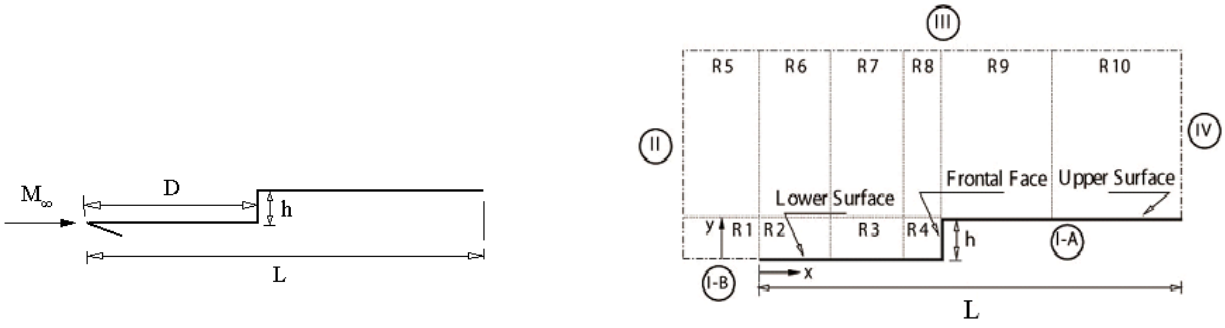

(a) **Forward-facing step** (b) **Computational domain**

Figure 1. Drawing illustrating (a) a schematic view of the forward-facing step and (b) the computational domain.

According to Fig. 1(a), M_∞ represents the freestream Mach number, h is the frontal-face height, L refers to the total length of the forward-facing step, and D stands for the location of the step. It was considered that the forward-facing step is infinitely long but only the length L is considered. It was assumed a frontal-face height h of 3, 6, and 9 mm, which correspond to $H = h/\lambda_\infty$ of 3.23, 6.46, and 9.69, D/λ_∞ of 50 and L/λ_∞ of 100, where λ_∞ is the freestream mean free path.

3. FREESTREAM AND FLOW CONDITIONS

Freestream and flow conditions employed in the present calculations are those defined in the previous studies (Leite and Santos, 2009a,b) and listed in Tab. 1, and the gas properties (Bird, 1994) considered in the simulation are shown in Tab. 2.

Table 1. Freestream flow conditions

Altitude (km)	T_∞(K)	p_∞(N/m^2)	ρ_∞(kg/m^3)	μ_∞(Ns/m^2)	n_∞(m^{-3})	λ_∞(m)
70	219.69	5.582	8.753×10^{-5}	1.455×10^{-5}	1.8192×10^{21}	9.285×10^{-4}

The freestream velocity U_∞ is assumed to be constant at 1485.3 m/s, 4527.8 m/s, and 7546.5 m/s, which corresponds

to a freestream Mach number M_∞ of 5, 15 and 25, respectively. The wall temperature T_w is assumed constant at 880 K. This temperature is chosen to be representative of the surface temperature near the stagnation point of a reentry vehicle and is assumed to be uniform over the forward-facing step surface.

By assuming the frontal-face height h as the characteristic length, the Knudsen number Kn_h corresponds to 0.3095, 0.1548 and 0.1032 for height h of 3, 6 and 9 mm, respectively. Finally, the Reynolds number Re_h, also based on the frontal-face height h and on conditions in the undisturbed stream, cover from 27 to 409 for the cases investigated.

Table 2. Gas properties

	X	m (kg)	d (m)	ω
O_2	0.237	5.312×10^{-26}	4.01×10^{-10}	0.77
N_2	0.763	4.650×10^{-26}	4.11×10^{-10}	0.74

4. COMPUTATIONAL METHOD AND PROCEDURE

The Direct Simulation Monte Carlo (DSMC) method, introduced by Bird (1994), has been found remarkably successful for predicting and understanding a number of difficult problems in rarefied gas dynamics. In the DSMC method, the gas is modeled at the microscopic level by using simulated particles. Each simulated particle represents a very large number of physical molecules or atoms. These representative molecules are tracked in the computer as they move, collide and undergo boundary interactions in the simulated physical space. In addition, the molecular motion is considered to be deterministic, and the intermolecular collisions are considered to be stochastic. Furthermore, these two processes are uncoupled over the small time step used to advance the simulation, and computed sequentially. The simulation is always calculated as an unsteady flow. However, a steady flow solution is obtained as the large time state of the simulation.

In the present account, collisions are simulated with the variable hard sphere (VHS) molecular model (Bird, 1981), and the no time counter (NTC) collision sampling technique (Bird, 1989). Repartition energy among translational and internal modes is controlled by the Borgnakke-Larsen statistical model (Borgnakke and Larsen, 1975). For the present work, the simulations are performed using a non-reacting gas model for a constant freestream gas composition consisting of 76.3% of N_2 and 23.7% of O_2, while considering energy exchange between translational, rotational and vibrational modes.

5. COMPUTATIONAL DOMAIN AND GRID

In order to implement the particle-particle collisions, the flowfield around the forward-facing step is divided into ten regions, which are subdivided into computational cells. The cells are further subdivided into subcells, two subcells/cell in each coordinate direction. This physical space network is used to facilitate the choice of molecules for collisions and for the sampling of the macroscopic flow properties such as density, velocity, pressure, temperature, etc.

A schematic view of the computational domain is depicted in Fig. 1(b). According to this figure, side I-A is defined by the forward-facing step surface. Diffuse reflection with complete thermal accommodation is the condition applied to this side. In a diffuse reflection, the molecules are reflected equally in all directions, and the final velocity of the molecules is randomly assigned according to a half-range Maxwellian distribution determined by the wall temperature. Side I-B represents a plane of symmetry, where all flow gradients normal to the plane are zero. At the molecular level, this plane is equivalent to a specular reflecting boundary. Sides II and III are the freestream side through which simulated molecules enter and exit. Depending on the case investigated, side II is positioned from $5\lambda_\infty$ to $10\lambda_\infty$ upstream of the flat-plate leading edge, and side III defined from $30\lambda_\infty$ to $52\lambda_\infty$ above the step upper surface. Finally, the flow at the downstream outflow boundary, side IV, is predominantly supersonic and vacuum condition is specified (Bird, 1994). At this boundary, simulated molecules can only exit.

DSMC results depend on the cell size chosen, on the time step as well as on the number of particles per computational cell. In the DSMC code, the linear dimensions of the cells should be small in comparison with the length scale of the

macroscopic flow gradients normal to the streamwise directions, which means that the cell dimensions should be the order of or smaller than the local mean free path (Alexander *et al.*, 1998, 2000). The time step should be chosen to be sufficiently small in comparison with the local mean collision time (Garcia and Wagner, 2000; Hadjiconstantinou, 2000). Finally, the number of simulated particles has to be large enough to make statistical correlations between particles insignificant.

As part of the verification process, a grid independence study was made with three different structured meshes, coarse, standard and fine, in each coordinate direction. The effect of altering the cell size in the x- and y-directions was investigated for a coarse and fine grids with, respectively, 50% less and 100% more cells with respect to the standard grid. As a base of comparison, for the M_∞ = 25 case, and for frontal-face height H of 3.23, 6.46, and 9.69, the total number of cells corresponded, respectively, to 20,000, 33,800, and 41,600 cells.

A discussion of the verification process, effects of cell size, time step and number of molecules on the aerodynamic surface quantities for the forward-facing steps presented herein, is described in detail in Leite (2009). Furthermore, as part of the validation process, results for density, velocity and translational temperature were compared with those obtained from other established DSMC code and experimental data in order to ascertain how well the DSMC code employed in this study is able to predict hypersonic flow in a flat plate. Details of this comparison is also presented in Leite (2009).

6. COMPUTATIONAL RESULTS AND DISCUSSION

Having computed aerodynamic surface properties over a representative range of simulation parameters, it proves convenient to summarize the major features of the results. In this sense, the purpose of this section is to discuss and to compare differences on the aerodynamic surface properties due to variations on the step frontal-face height and on the freestream Mach number. For the time being, aerodynamic surface quantities of particular interest are number flux, pressure, heat transfer, and shear stress.

6.1 Number Flux

The number flux N is calculated by sampling the molecules impinging on the surface by unit time and unit area. The distribution of the number flux along the lower and upper surfaces, and on the frontal-face surface is illustrated in Figs. 2 and 3 as a function of the freestream Mach number M_∞ and parameterized by the dimensionless frontal-face height H. In this group of plots, the dimensionless number flux N_f represents the number flux N normalized by $n_\infty U_\infty$, where n_∞ is the freestream number density and U_∞ is the freestream velocity. It is important to recall that U_∞ is different for each Mach number case investigated. In addition, X and Y are the lengths x and y normalized by the freestream mean free path λ_∞. As a basis of comparison, the dimensionless number flux for the flat-plate case is also illustrated in the plot for freestream Mach number of 25.

Looking first to Fig. 2, it is clearly noticed that the number flux to the surface depends on the frontal-face height H as well as on the freestream Mach number M_∞. It is seen that the number flux N_f increases with increasing the frontal-face H and with the freestream Mach number M_∞. In general, close to the sharp leading edge, the behavior of the number flux to the lower surface is similar to that for the flat-plate case. This is an expected behavior since the flow in this region is not affected by the presence of the step. As the flow develops downstream along the lower surface, the presence of the step is felt in the number flux distribution, since N_f dramatically increases in comparison to the number flux observed for the flat-plate case, Fig. 2(c). For the M_∞ = 25 case, the presence of the step is felt in the number flux at section X corresponding to approximately 32.6, 38.1 and 43.4, for frontal-face height H of 9.69, 6.46, and 3.23, respectively. From these sections up to the section where the steps are located, X = 50, the number flux to the lower surface dramatically increases in comparison to the number flux observed for the flat-plate case.

Of particular interest is the number flux behavior at the vicinity of the step base. This region, where a significant number-flux rise is observed, is directly related to the recirculation zone that forms ahead of the step frontal face (Leite, 2009). The recirculation zone concentrates a large number of molecules. The molecules enclosed in this region, when

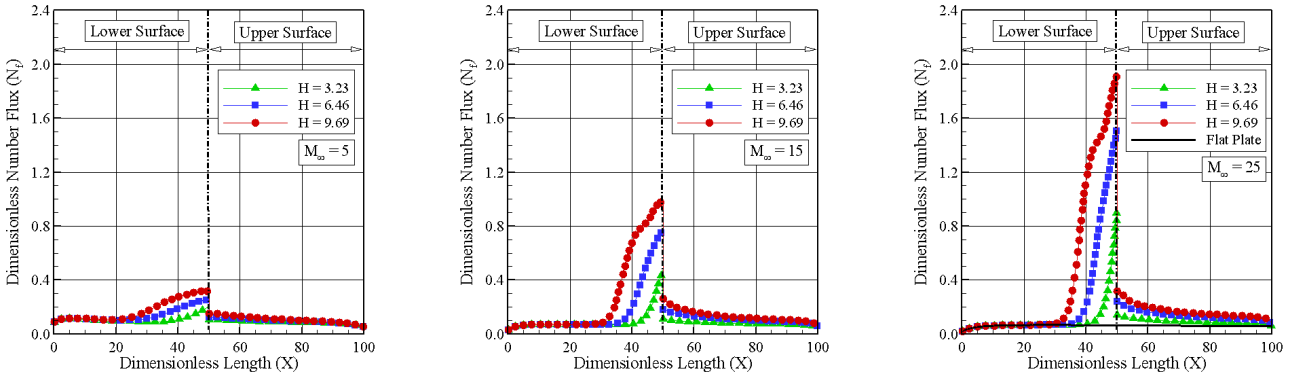

Figure 2. Dimensionless number flux distribution along the lower and upper surfaces for freestream Mach number of 5 (left), 15 (middle), and 25 (right).

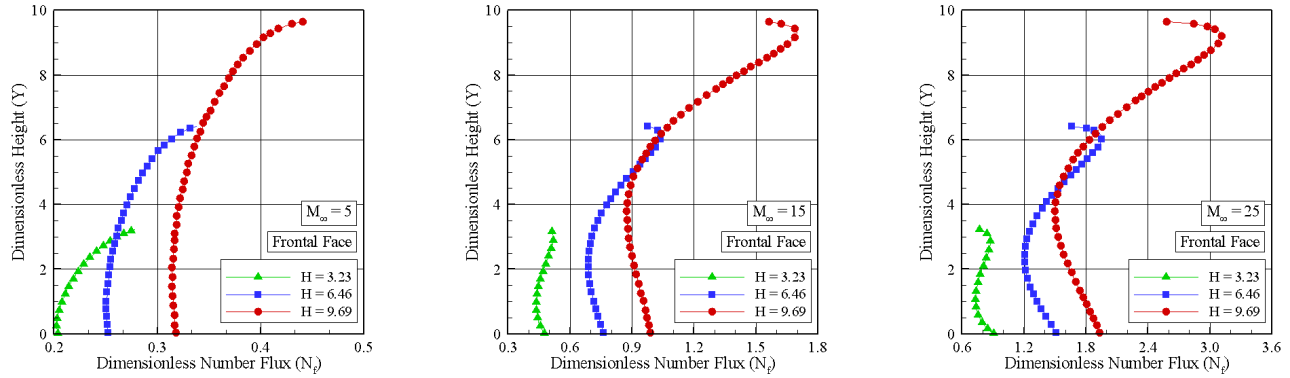

Figure 3. Dimensionless number flux distribution along the frontal-face surface for freestream Mach number of 5 (left), 15 (middle), and 25 (right).

colliding with the lower and frontal-face surfaces, increase not only the number flux to both surfaces but also the energy exchange as well as the linear momentum, as will be seen subsequently.

Turning next to Fig. 3, it can be seen that the number flux to the frontal-face surface is more intense than that observed to the lower surface. Similar to that for the lower surface, the number flux to the frontal face is a function of the step height H and of the freestream Mach number M_∞, i.e, it increases with both the frontal-face height and with freestream Mach number rise. It may be recognized from this figure that the number flux distribution presents a peak value at the vicinity of the step corner for the M_∞ of 15 and 25. For the M_∞ = 25 case, the peak value takes place at section Y equal to 2.83, 6.09, and 9.21 for H of 3.23, 6.46, and 9.69, respectively. As a matter of fact, the flow reattachment point, Y_r, on the frontal face occurs for section Y equal to 2.69, 5.66 and 8.72 for H of 3.23, 6.46, and 9.69, respectively. It is important to mention that the flow reattachment point on the frontal-face of the step was obtained by calculating the section where the shear stress τ_w changes from negative value to positive one, i.e., $\tau_w = 0$.

6.2 Heat Transfer Coefficient

The heat flux q_w to the body surface is calculated by the net energy flux of the molecules impinging on the surface. A flux is regarded as positive if it is directed toward the body surface. The net heat flux q_w is related to the sum of the translational, rotational and vibrational energies of both incident and reflected molecules as defined by,

$$q_w = q_i - q_r = \frac{F_N}{A\Delta t}\{\sum_{j=1}^{N}[\frac{1}{2}m_j c_j^2 + e_{Rj} + e_{Vj}]_i - \sum_{j=1}^{N}[\frac{1}{2}m_j c_j^2 + e_{Rj} + e_{Vj}]_r\} \quad (1)$$

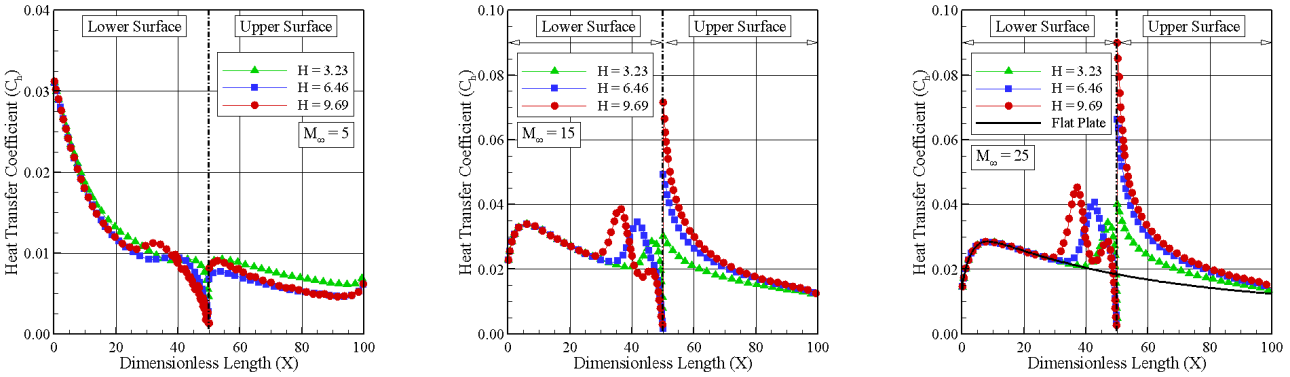

Figure 4. Heat transfer coefficient distribution along the lower and upper surfaces for freestream Mach number of 5 (left), 15 (middle), and 25 (right).

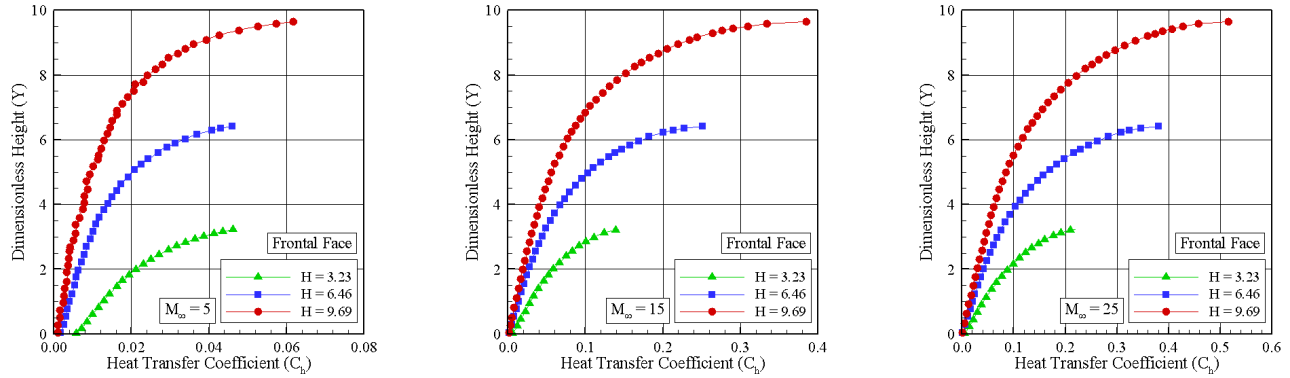

Figure 5. Heat transfer coefficient distribution along the frontal-face surface for freestream Mach number of 5 (left), 15 (middle), and 25 (right).

where F_N is the number of real molecules represented by a single simulated molecule, N is the number of molecules colliding with the surface by unit time and unit area, Δt refers to the time step, A is the area, m is the mass of the molecules, c is the velocity of the molecules, e_R and e_V stand for the rotational and vibrational energies, respectively. Subscripts i and r refer to incident and reflect molecules. In addition, the heat transfer coefficient C_h is the heat flux q_w normalized by the dynamic energy defined by $\rho_\infty U_\infty^3/2$.

The dependence of the heat transfer coefficient C_h on the frontal-face height H and on the freestream Mach number M_∞ is demonstrated in Fig. 4 for the lower and upper surfaces, and in Fig. 5 for the frontal-face surface. According to Fig. 4, important features can be observed in the heat transfer coefficient behavior. Of particular interest, it is seen that the heat transfer distribution for M_∞ = 5 case differs from that for the other two cases in the sense that it is high at the sharp leading edge and decreases along the lower surface. In contrast, for freestream Mach number of 15 and 25, the heat transfer coefficient C_h follows the same behavior presented by the flat-plate case close to the sharp leading edge, region unaffected by the presence of the steps. Further downstream along the lower surface, the heat transfer coefficient C_h significantly increases and reaches pick values close to the frontal face, then decreases to almost zero at the stagnation region. Along the upper surface, the heat transfer coefficient presents a maximum value at the step corner and then decreases downstream along the surface, basically reaching the values observed for the flat-plate case.

Referring to Fig. 5, along the frontal-face surface, the heat transfer coefficient increases monotonically, from zero at the stagnation point to a maximum value near the step corner, which depends on the frontal-face height h and on the freestream Mach number. It is quite apparent that this significant increase in the heat transfer coefficient is due to the flow reattachment zone. In addition, for freestream Mach number of 15 and 25, the maximum values observed for the heat transfer coefficient on the frontal-face surface is an order of magnitude greater than those observed on the lower surface. For comparative purpose, for the M_∞ = 25 case, the maximum values for C_h are around 0.22, 0.38 and 0.52 for height

H of 3.23, 6,46 and 9.69, respectively. In contrast, the C_h for the flat-plate case, i.e., a flat plate without steps, is around 0.0284 at section X = 9.11 in the lower surface. Therefore, C_h of 0.22, 0.38 and 0.52 correspond respectively to 7.75, 13.38 and 18.31 times the pick value for the flat-plate case. Furthermore, it is very encouraging to observe that, for the H = 9.69 case, the amount of energy transferred to the step corner represents around 50% of the total energy ($\rho_\infty U_\infty^3/2$) of the gas coming from the freestream.

6.3 Pressure Coefficient

The pressure p_w on the body surface is calculated by the sum of the normal momentum fluxes of both incident and reflected molecules at each time step as follows,

$$p_w = p_i - p_r = \frac{F_N}{A\Delta t}\sum_{j=1}^{N}\{[(mv)_j]_i - [(mv)_j]_r\} \tag{2}$$

where v is the velocity component of the molecule j in the surface normal direction. The pressure coefficient C_p is p_w-p_∞ normalized by the dynamic pressure, $\rho_\infty U_\infty^2/2$.

The impact on the pressure coefficient C_p caused by changes on the frontal-face height h and on the freestream Mach number is depicted in Fig. 6 for lower and upper surfaces, and in Fig. 7 for frontal-face surface. According to this group of plots, it is noted that the pressure coefficient behavior follows the same trend as that shown for the number flux in the sense that the maximum values for C_p along the the lower surface occur at the stagnation point, at the lower-surface/frontal-face junction. Along the frontal-face surface, the peak value for C_p occurs close the frontal-face/upper-surface junction, similar

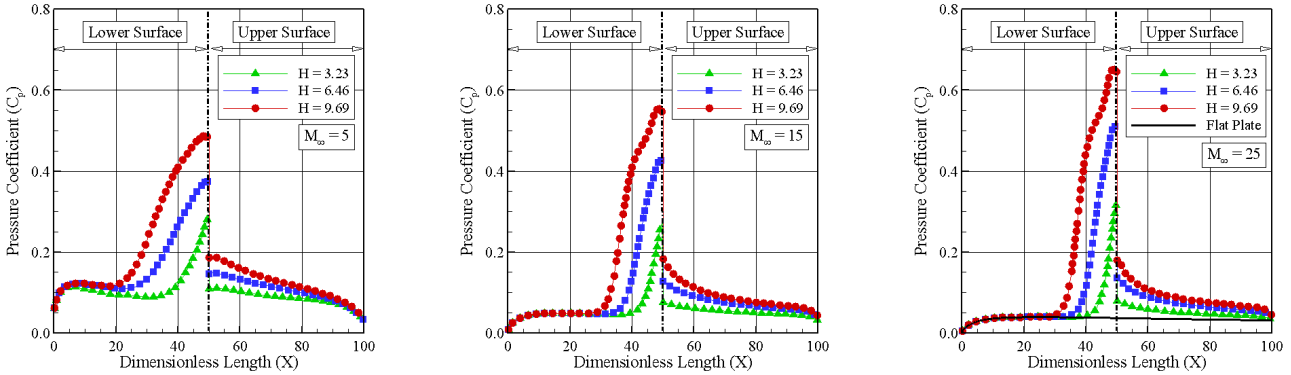

Figure 6. Pressure coefficient distribution along the lower and upper surfaces for freestream Mach number of 5 (left), 15 (middle), and 25 (right).

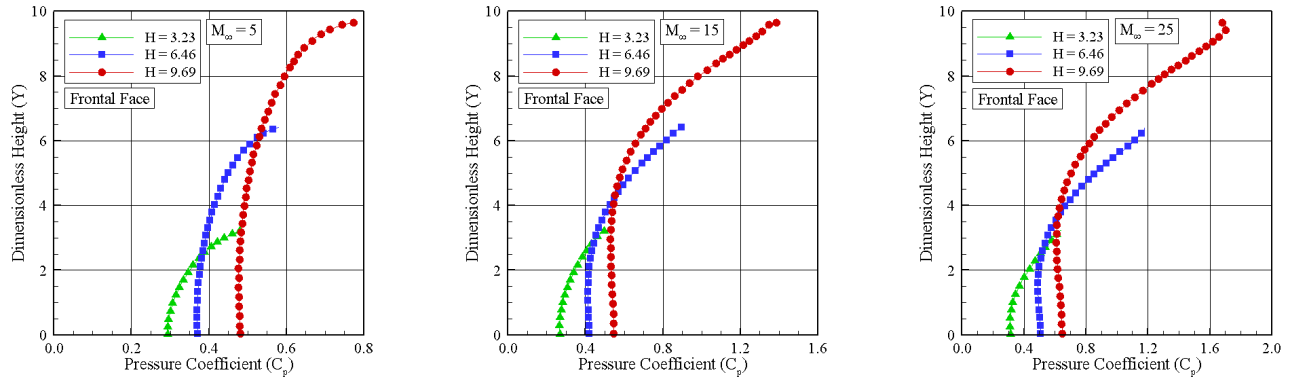

Figure 7. Pressure coefficient distribution along the frontal-face surface for freestream Mach number of 5 (left), 15 (middle), and 25 (right).

to that peak value location for the heat transfer coefficient. In addition, for M_∞ = 25 case, pressure coefficient behavior along the step surface is similar to that for the flat-plate case at the vicinity of the sharp leading edge. The upstream disturbances in the pressure coefficient C_p, due to the presence of the step, were felt up to section X corresponding to approximately 32.6, 38.1, and 43.4 for steps with height H of 9.69, 6.46, and 3.23, respectively. Furthermore, from these sections to the step position, X = 50, the pressure coefficient C_p increases dramatically when compared to that for the flat-plate case.

For comparison purpose, the maximum values for C_p on the frontal face are around 0.64, 1.17 and 1.68 for height H of 3.23, 6,46 and 9.69, respectively. In contrast, the maximum value of C_p for the flat-plate case, i.e., a flat plate without steps, is around 0.0393 at section X = 25.96 in the lower surface. Therefore, C_p of 0.64, 1.17 and 1.68 correspond respectively to 16.28, 29.77 and 42.75 times the pick value for the flat-plate case, which corresponds to a smooth surface.

6.4 Skin Friction Coefficient

The shear stress τ_w on the body surface is calculated by the sum of the tangential momentum fluxes of both incident and reflected molecules impinging on the surface at each time step by the following expression,

$$\tau_w = \tau_i - \tau_r = \frac{F_N}{A\Delta t}\sum_{j=1}^{N}\{[(mu)_j]_i - [(mu)_j]_r\} \tag{3}$$

where u is the velocity component of the molecule j in the surface tangential direction. Nevertheless, for the special case of diffuse reflection, the gas-surface interaction model adopted herein, the reflected molecules have a tangential momentum equal to zero, since molecules essentially lose, on average, their tangential velocity components. In this fashion, the tangential momentum flux of the molecules is defined as follows,

$$\tau_w = \tau_i = \frac{F_N}{A\Delta t}\sum_{j=1}^{N}\{[(mu)_j]_i\} \tag{4}$$

In addition, the skin friction coefficient C_f is defined as being the shear stress τ_w normalized by the dynamic pressure, $\rho_\infty U_\infty^2/2$.

The distribution of skin friction coefficient C_f along the step surfaces – lower, upper, and frontal face – is displayed in Figs. 8 and 9 as a function of the step height H and freestream Mach Number M_∞. Once again, in this set of plots, X and Y represent, respectively, the lengths x and y normalized by the freestream mean free path λ_∞.

Based on Fig. 8, it is observed that the skin friction coefficient distribution for M_∞ = 5 case differs from that for the

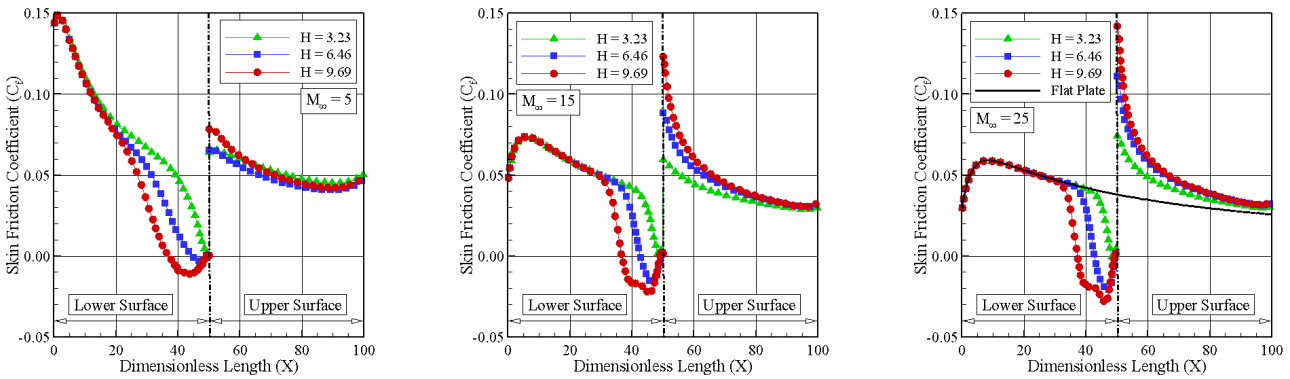

Figure 8. Skin friction coefficient distribution along the lower and upper surfaces for freestream Mach number of 5 (left), 15 (middle), and 25 (right).

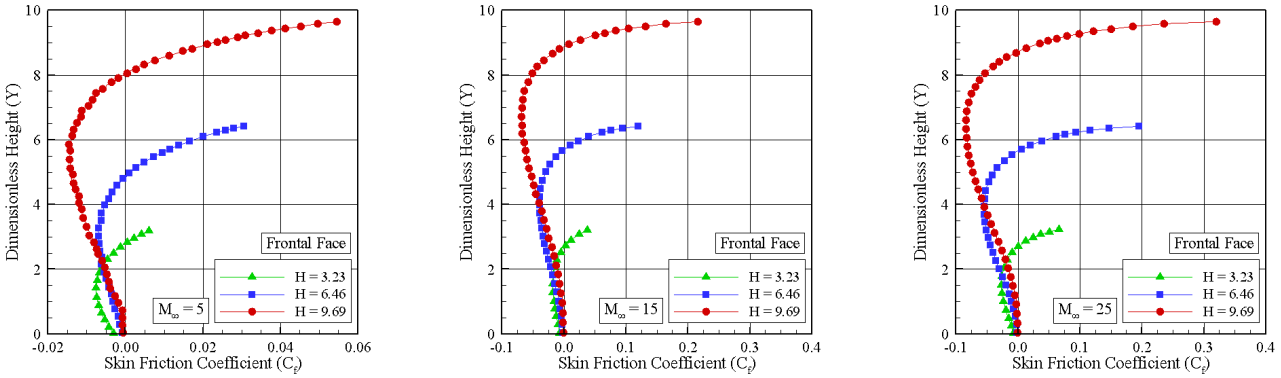

Figure 9. Skin friction coefficient distribution along the frontal-face surface for freestream Mach number of 5 (left), 15 (middle), and 25 (right).

other two cases in the sense that it is high at the sharp leading edge and decreases along the lower surface. Conversely, for freestream Mach number of 15 and 25, the skin friction coefficient C_f follows the same behavior of that given by the flat-plate case up to a certain distance from the step. From this position to the step position, $X = 50$, the skin friction coefficient C_f decreases, when compared to that for the flat-plate case, and reaches negative values. After that, as a result of the recirculation region, the skin friction coefficient C_f continues to decrease up to a minimum point. After the minimum point, C_f increases again and reaches values close to zero at the stagnation point at the base of the step. Along the upper surface, the skin friction coefficient C_f presents the maximum value at the step shoulder, then drops off downstream and reaches the value observed for the flat-plate case.

Turning to Fig. 9, along the frontal face, the skin friction coefficient C_f is basically zero at the step base. After that, it stays negative from the step base up to the flow reattachment point. From this point up to the step corner, the skin friction coefficient drastically increases, since this is basically a region exposed to a high speed flow. Afterwards, due to the flow expansion around the step corner, the skin friction coefficient C_f diminishes by approximately 50% in comparison to the values observed at the beginning of the upper surface. It should be mentioned that the section corresponding to the condition of $C_f = 0$ ($\tau_w = 0$) was used to define the separation point.

7. CONCLUDING REMARKS

A computational investigation has been carried out for the hypersonic flow over forward-facing steps in the transition flow regime. The main focus was to analyze the impact of the freestream Mach number and the step frontal-face hight on the aerodynamic surface quantities. Effects of compressibility on heat transfer, pressure, and skin friction coefficients were investigated for a representative range of parameters. The freestream Mach number varied from 5 to 25. In addition, the step frontal-face height ranged from 3 to 9 millimeters, which corresponded overall Knudsen numbers from 0.3095 to 0.1032. Therefore, these cases covered the hypersonic flow in the transitional flow regime.

The analysis showed that changes on the freestream Mach number affected the surface quantities along the lower and upper surfaces in a different way for the range considered in this work. It was found that the behavior of heat transfer, pressure, and skin friction coefficients presented for freestream Mach number of 5 is different from those for freestream Mach number of 15 and 25. In contrast, no significant differences were observed in the behavior of heat transfer, pressure and skin friction coefficients along the step frontal face for the range of freestream Mach number investigated.

8. ACKNOWLEDGEMENTS

The authors would like to thank the financial support provided by CNPq (Conselho Nacional de Desenvolvimento Científico e Tecnológico) under Grant No. 473267/2008-0, and by FAPESP (Fundação de Amparo a Pesquisa do Estado de São Paulo) under Grant No. 2012/19325-4.

9. REFERENCES

Alexander, F. J., Garcia, A. L., and Alder, B. J., 1998. "Cell size dependence of transport coefficient in stochastic particle algorithms". *Physics of Fluids*, Vol. 10, pp. 1540–1542.

Alexander, F. J., Garcia, A. L., and Alder, B. J., 2000. "Erratum: Cell size dependence of transport coefficient in stochastic particle algorithms". *Physics of Fluids*, Vol. 12, pp. 731–731.

Bird, G. A., 1981. "Monte Carlo simulation in an engineering context". In Fisher, S. S., ed., *Progress in Astronautics and Aeronautics: Rarefied gas Dynamics*, Vol. 74, part I, AIAA New York, pp. 239–255.

Bird, G. A., 1989. "Perception of Numerical Method in Rarefied Gasdynamics". In Muntz, E. P., Weaver, D. P., and Capbell, D. H., eds., *Rarefied Gas Dynamics: Theoretical and Computational Techniques*, Vol. 118, Progress in Astronautics and Aeronautics, AIAA, New York, pp. 374–395.

Bird, G. A., 1994. *Molecular gas dynamics and the direct simulation of gas flows*, Oxford University Press.

Bogdonoff, S. M. and Kepler, C. E., 1955. "Separation of a supersonic turbulent boundary layer". *Journal of The Aeronautical Science*, Vol. 22, pp. 414–430.

Borgnakke, C. and Larsen, P. S., 1975. "Statistical collision model for Monte Carlo simulation of polyatomic gas mixture". *Journal of Computational Physics*, Vol. 18, pp. 405–420.

Camussi, R., Felli, M., Pereira, F., Aloisio, G., and DiMarco, A., 2008. "Statistical properties of wall pressure fluctuations over a forward-facing step". *Physics of Fluids*, Vol. 20, 075113.

Chapman, D. R., Kuehn, D. M., and Larson, H. K., 1958. "Investigation of separeted flows in supersonic and subsonic streams with emphasis on the effect of transition". NACA Report 1356.

Driftmyer, R. T., 1973. "A forward facing step study: the step height less than the boundary-layer thickness". NOLTR 73-98, Naval Ordinance Laboratory, White Oak, Maryland.

Garcia, A. L., and Wagner, W., 2000. "Time Step Truncation Error in Direct Simulation Monte Carlo". *Physics of Fluids*, Vol. 12, pp. 2621–2633.

Grotowsky, M. G., and Ballmann J., 2000. "Numerical investigation of hypersonic step-flows". *Shock Waves*, Vol. 10, pp. 57–72.

Hadjiconstantinou, N. G., 2000. "Analysis of Discretization in the Direct Simulation Monte Carlo". *Physics of Fluids*, Vol. 12, pp. 2634–2638.

Leite, P. H. M., and Santos, W. F. N., 2009a. "Direct Simulation of Low Density Hypersonic Flow over a Foward-Facing Step". In *20th International Congress of Mechanical Engineering*, COBEM 2009, November 15–20, Gramado, RS, Brazil.

Leite, P. H. M., and Santos, W. F. N., 2009b. "Numerical Investigation of Heat Transfer and Pressure Distribution of Hypersonic Flow over a Forward-Facing Step". In *30th Iberian-Latin-American Congress on Computational Methods in Engineering*, CILAMCE 2009, November 5–8, Armação de Búzios, RJ, Brazil.

Leite, P. H. M, 2009. "Direct Simulation of the Step Influence on a Reentry Vehicle Surface (in Portuguese)". MS Dissertation, INPE.

Nestler, D. E., Saydah, A. R., and Auxer, W. L., 1969. "Heat transfer to steps and cavities in hypersonic turbulent flow". *AIAA Journal*, Vol. 7, pp. 1368–1370.

Stüer, H., Gyr, A., and Kinzelbach, W., 1999. "Laminar separation on a forward facing step". *Eur. J. Mech. B/Fluids*, Vol. 18, pp. 675–6920.

Wilkinson, P. R. and East, R. A., 1968. "Mean properties of a region of separation in laminar hypersonic flow". *AIAA Journal*, Vol. 6, pp. 2183–2184.

10. RESPONSIBILITY NOTICE

The authors are the only responsible for the printed material included in this paper.